Enhancing LoRa Capacity using Non-Binary Single Parity Check Codes

Tallal Elshabrawy
Faculty of Information Engineering & Technology
German University in Cairo, Egypt
tallal.el-shabrawy@guc.edu.eg

Joerg Robert
Lehrstuhl fur Informationstechnik (Kommunikationselektronik)
Friedrich-Alexander Universitat Erlangen-Nurnberg, Germany
joerg.robert@fau.de

***Abstract*—LoRa has established itself as one of the main solutions within evolving Low Power Wide Area Networks, LP-WAN. LoRa is primarily pillared on its patented chirp spread spectrum modulation. In LoRa modulation, linearly increasing cyclic chirp signals span the LoRa bandwidth. The rate of increase of these chirp signals is dependent on the applied spreading factor (SF). Increasing the spreading factor extends the coverage range for LoRa communication at the expense of a reduced data rate. Typically, LoRa signals with different spreading factors are quasi-orthogonal such that LoRa essentially supports multiple simultaneous logical networks with different coverage ranges. Given that LoRa utilizes an ALOHA-based protocol for medium access, the total capacity of LoRa networks is governed by the system loads and time-on-air for packet transmissions of each SF-network. In this paper, non-binary single parity check (SPC) codes with soft-decision decoding are introduced as a tool to enhance the capacity of LoRa networks. The LLRs for the soft decision decoding of LoRa symbols are first derived. It is then shown that SPC codes succeed in achieving measurable coding gains for typical LP-WAN applications at the scale of 1.2 dB. Coinciding with enabling/disabling SPC in each logical SF-network, the system loads as well as the packet transmission times could be optimized with the objective of maximizing the packet delivery ratio. The presented capacity results indicate that in fact SPC optimization can achieve capacity gains at the scale of up to 65% compared to the nominal LoRa networks.**

***Index Terms*—LP-WAN, LoRa Capacity, Chirp Modulation, SF-Allocation, Non-Binary Single Parity Check Codes.**

I. Introduction

Realization of a multitude of IoT applications, particularly within smart cities, envisions deployment over Low Power Wide Area Networks (LP-WAN) [1]. LP-WAN are typically configured as star-of-star networks. Within each underlying star network, thousands of energy-constrained IoT devices communicate directly with an IoT gateway over long distances at the scale of kilometers [1]. Recently, LoRa has been exhibiting tremendous commercial growth to establish itself among the front runners of emerging LP-WAN. LoRa is primarily pillared on its patented chirp spread spectrum modulation that supports energy-efficient/reliable long-range communication. In LoRa modulation, linearly increasing cyclic chirp signals span the LoRa bandwidth. Rate of increase of these chirp signals is dependent on the applied spreading factor that ranges between 7 and 12. Increasing the spreading factor extends coverage range for LoRa communication at the expense of a reduced data rate. LoRa signals with different spreading factors are quasi-orthogonal such that LoRa supports multiple simultaneous logical networks [2].

The scale of aggregate traffic load to be generated by dense IoT applications constitutes a significant challenge for evolving LoRa networks. Therefore, scalability of LoRa capacity in conjunction with the adopted simple ALOHA-based medium access scheme has been thoroughly investigated in the literature [3], [4], [5], [6]. Moreover, some recent research activities have been directed towards spreading factor (SF) allocation as a vehicle to enhance LoRa capacity [5], [7], [8]. By the merit of different sensitivities supported by each spreading factor, LoRa networks could be organized into multiple coverage tiers. Within each tier, the spreading factor coinciding with the tier coverage range as well as all other higher spreading factors can be considered available for allocation. In conjunction with the vulnerability of ALOHA to longer packet durations, it is intuitively favorable to assign an end device with the least spreading factor available for allocation at the device's coverage location [5]. Nevertheless, such strategy overlooks impact of system loads of each individual logical SF-network on the attainable total LoRa capacity. In [7], two SF-allocation strategies are proposed with the objective of balancing the loads across the LoRa SF-networks. On the other hand, the work in [8] has formulated an optimization problem for SF-allocation. The proposed strategy determines the SF-network tiers based on assignment distances derived from the solution of the optimization problem rather than coverage distances derived from the physical layer LoRa sensitivities. The work to be presented in this paper introduces a new dimension to the SF-allocation problem. Forward error correction (FEC) is utilized as a tool to control coverage sensitivities, system loads and time-on-air of individual SF-networks with the objective of maximizing the aggregate LoRa capacity. In particular, simple, high rate non-binary single-parity check (SPC) codes are proposed for LoRa. The LLRs for soft decision decoding of LoRa symbols are derived. It is shown that such SPC codes succeed in achieving measurable coding gains at the scale of 1.2 dB when deployed for payloads of typical LP-WAN applications. The high rate of SPC guarantees that coding gain is associated with minimal penalty for the corresponding increase in the time-on-air. The impact of SPC on LoRa capacity is then investigated. SPC optimization across all the logical SF-networks could be deployed to design the compromise between varying sensitivities and time-on-air. It is shown that SPC optimization could possibly increase the LoRa network capacity by up to 65%. It is to be noted that FEC using convolutional fountain-like codes has been proposed for improving LoRa packet delivery ratio in [9]. However, the considered FEC has been applied at the application layer with coding rates down to 0.5 where the impact of increase of packet sizes on the LoRa capacity has not been evaluated.

The rest of the paper is organized as follows. In Section II, theoretical description of LoRa modulation and nominal LoRa FEC are reviewed. Soft decision LLR for SPC are derived and the SPC decoding scheme are presented in Section III. Section IV shows the capacity gains projected using SPC optimization. Finally, Section V is dedicated for conclusions.

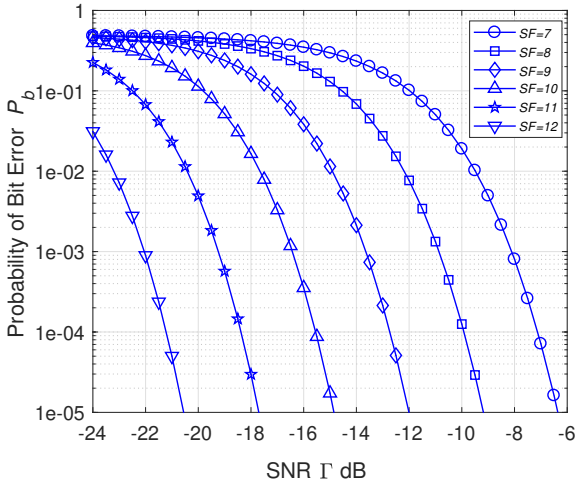

Fig. 1. LoRa BER Performance at different Spreading Factors SF.

II. Basics of LoRa Physical Layer

A. LoRa Modulation

LoRa adopts a frequency shift chirp modulation scheme [10]. Consider a LoRa system in the baseband where the chirp signal frequency has bandwidth B. Consequently, one LoRa sample is transmitted every $T = 1/B$. LoRa modulation is achieved by spreading the frequency change of the chirp signal across 2^{SF} samples within a symbol duration of $T_S = 2^{SF} \times T$, where $SF \in \{7, 8, ..., 12\}$ depicts the spreading factor. Let $\omega_0(nT)$ depict a basis chirp signal whose frequency increases linearly between 0 and bandwidth B. Accordingly, $\omega_0(nT)$ could be expressed as

$$\omega_0(nT) = \sqrt{\frac{1}{2^{SF}}} \exp\left[j2\pi(\frac{nB}{2^{SF}}) \cdot .nT\right] = \sqrt{\frac{1}{2^{SF}}} \exp\left[j2\pi(n) \cdot \frac{n}{2^{SF}}\right], \quad (1)$$

where $n = 0, 1, 2, \ldots, 2^{SF} - 1$ depicts the sample index at time nT. For each spreading factor SF in LoRa, 2^{SF} non-binary symbols $s_k = k$, $k \in \{0, 1, 2, \ldots, 2^{SF} - 1\}$ are transmitted using the k^{th} cyclic frequency shift of $\omega_0(nT)$ around the bandwidth B. Accordingly, LoRa specifies a total of 2^{SF} basis chirp signals $\omega_k(nT)$ given as

$$\omega_k(nT) = \sqrt{\frac{1}{2^{SF}}} \exp\left[j2\pi(k+n) \mod 2^{SF} \cdot \frac{n}{2^{SF}}\right]. \quad (2)$$

From (2), it is evident that each LoRa symbol s_k is characterized by a frequency offset $f_k = B{\cdot}k/2^{SF}$ that sets the starting frequency of the corresponding chirp signal. LoRa demodulation is founded on the orthogonality of the underlying chirp basis signals [10], where the cross-correlation properties between the 2^{SF} possible LoRa basis signals are governed by

$$\mathcal{C}_{l,k} = \sum_{n=0}^{2^{SF}-1} \omega_l(nT) \cdot \omega_k^*(nT) = \begin{cases} 1 & k = l \\ 0 & k \neq l \end{cases}, \quad (3)$$

where $\mathcal{C}_{l,k}$ depicts the cross-correlation between basis chirp signals $\omega_l(nT)$, $\omega_k(nT)$ $\forall l, k \in \{0, 1, \ldots, 2^{SF} - 1\}$ and $\omega_k^*(nT)$ depicts the complex conjugate of the basis function $\omega_k(nT)$.

Without loss of generality, let us focus on the transmission of the LoRa symbol $s_0 = 0$ using the basis chirp signal $\omega_0(nT)$ over an AWGN channel. The correlator output $\mathcal{R}_0$ for a received signal $r_0(nT)$ that corresponds to a transmitted symbol $s_0 = 0$ at the LoRa demodulator is given as

$$\mathcal{R}_0 = \sum_{n=0}^{2^{SF}-1} r_0(nT) \cdot \omega_k^*(nT) = \begin{cases} \sqrt{E_S} + \eta_0 & k = 0 \\ \eta_k & k \neq 0 \end{cases}, \quad (4)$$

where E_S is the symbol energy and $\eta_k, \forall k \in \{0, 1, 2, \ldots, 2^{SF} - 1\}$ depicts a complex Gaussian noise process.

The detection of LoRa symbols reverts to selection of the index of the LoRa basis signal with the highest correlation magnitude with the received signal. Therefore, for the received waveform $r_0(nT)$ corresponding to a transmitted symbol $s_0 = 0$, the detected symbol $d \in \{0, 1, \ldots, 2^{SF} - 1\}$ is computed as

$$d = \arg_k \max\left(\left|\delta_{0,k}\sqrt{E_S} + \eta_k\right|\right), \quad (5)$$

where, $\delta_{0,k} = 1$ for $k = 0$ and $\delta_{0,k} = 0$ otherwise.

Let us define $\rho_k = |\eta_k|$ as the magnitude of the complex noise envelope. Given that η_k is a complex zero-mean Gaussian noise process, then ρ_k depicts a Rayleigh distributed random variable with the cumulative distribution function

$$F_{\rho_k}(\rho) = 1 - \exp\left[-\frac{\rho^2}{2\sigma^2}\right], \quad (6)$$

where $\sigma^2 = N_0/2$ and N_0 is the single-sided noise power spectral density.

Let us define $P_{e|0}$ as the probability of symbol error given that symbol $s_0 = 0$ is transmitted. Given the outputs of the correlation process defined in (4), $P_{e|0}$ can be expressed as

$$P_{e|0} = \Pr\left[\max_{k,k\neq 0}(\rho_k) > \beta_0\right], \quad (7)$$

where $\beta_0 = \left|\sqrt{E_S} + \eta_0\right|$ and β_0 accordingly follows the Rician distribution with the shape parameter $\kappa_\beta = E_S/2\sigma^2 = E_S/N_0$.

Let $\hat{\rho} = \max_{k,k\neq 0}(\rho_k)$ depict a random variable for the maximum of $2^{SF} - 1$ i.i.d. Rayleigh random variables. The cumulative distribution function for $\hat{\rho}$ can be given as

$$F_{\hat{\rho}}(\rho) = \left[1 - \exp\left[-\frac{\rho^2}{2\sigma^2}\right]\right]^{2^{SF}-1}. \quad (8)$$

Given (7), (8) and assuming equally probable symbols, the average bit error probability P_b can be expressed as

$$P_b = 0.5 \times \int_0^\infty \left[1 - \left[1 - \exp\left[-\frac{\beta^2}{2\sigma^2}\right]\right]^{2^{SF}-1}\right] \cdot f_\beta(\beta) d\beta, \quad (9)$$

where $f_\beta(\beta)$ is the probability density function for the Rician distributed β. The multiplier of 0.5 before the integral indicates that for each symbol error only half of the underlying symbol bits are expected to be in error. This is attributed to the fact that the maximum noise amplitude $\hat{\rho}$ is equally likely to be associated with any of the $2^{SF} - 1$ noise bins at the correlator output. Figure 1 shows the numerical evaluation of the BER performance in (9) as a function of the SNR Γ that is related to E_S/N_0 using

$$\Gamma = \frac{E_s/T_S}{N_0 \cdot B} = \frac{E_S}{N_0 \cdot 2^{SF}}. \quad (10)$$

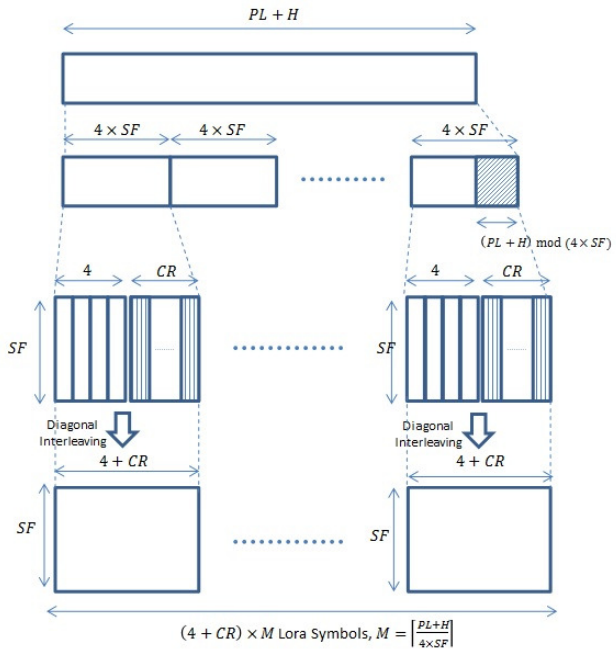

Fig. 2. FEC Encoding Process in LoRa.

B. LoRa FEC Hamming Code

LoRa communication may be considered vulnerable to two sources of erroneous detection; imperfect synchronization and noise-driven errors. Imperfect synchronization corresponds to time shifts that may result in the erroneous detection of the neighboring symbols to the one that has been actually transmitted. Accordingly, LoRa applies gray indexing in order to control that synchronization errors most likely correspond to single bit errors for each erroneous symbol. On the other hand as suggested by (7), noise-driven errors do not feature such single bit errors bias where all $2^{SF}-1$ candidate erroneous symbols are equally likely to occur. The gray indexing would not be of any help under such scenarios.

In order to cope with erroneous detection, the standard LoRa transceiver supports FEC on the basis of a simple binary Hamming code with rates $4/(4+CR)$ and $CR \in \{1,2,3,4\}$ [11], [12]. Figure 2 summarizes the corresponding encoding process till the representation of the encoded packet as LoRa symbols. As shown in the figure, the payload with PL bits along with the physical layer header of H bits are first subdivided into M blocks of length $4 \times SF$ bits each. The last block includes padded bits to adjust the appropriate block size. Each block is then organized into a matrix with SF rows and 4 columns. Dependent on the desired Hamming code rate, CR columns are appended with the parity bits. Accordingly, each block becomes constituted of SF codewords (rows) with each codeword encoded using a code rate of $4/(4+CR)$. A diagonal interleaver is then applied to evenly distribute the bits of each codeword over the SF rows of the matrix. Finally, each column of SF bits is transmitted as a LoRa symbol where the diagonal interleaver guarantees that no codeword maintains the same bit position across the $(4+CR)$ constructed symbols [11]. This is of significant importance such that imperfect synchronization leads to the minimum possible number of bit errors per codeword.

TABLE I
SENSITIVITY AND SNR FOR LORA WITH $B = 125\,\text{KHz}$, $CR = 1$.

SF	Data Rate (kb/s) [13]	Sensitivity (dBm) [13]	SNR (dB)
7	5.468	-123	-6
8	3.125	-126	-9
9	1.757	-129	-12
10	0.976	-132	-15
11	0.537	-134.5	-17.5
12	0.293	-137	-20

III. LoRa Capacity with Non-Binary SPC

A. SPC for LoRa Networks

The coding scheme presented in Figure 2 might be adequate to deal with imperfect synchronization. However when it comes to noise-driven errors, the binary Hamming codes adopted by LoRa are not known to exhibit any decent coding gains. The coding rates of $4/5$ and $4/6$ support error detection while the coding rates of $4/7$ and $4/8$ have the capability to correct a single bit error. In order to demonstrate the restricted capabilities of the Hamming codes in LoRa, Table I depicts the announced LoRa sensitivities operating within a bandwidth of $B = 125\,\text{KHz}$, and corresponding to a coding rate of $4/5$ as per [13]. The sensitivities from [13] are mapped to SNR in Table I using the relation $SNR = P_{Rx} + 174 - 10.\log_{10}(B) - NF$ where P_{Rx} is the receiver sensitivity and $NF = 6\,\text{dB}$ is the noise figure [13]. By comparing the SNR values in Table I against the BER curves in Figure 1, it is clear that the reported sensitivities coincide with the uncoded BER performance at the scale of $P_b = 10^{-5}$. Moreover, by inspecting [14][1], the more robust coding rates of $4/7$ and $4/8$ do not seem to be achieving any measurable sensitivity performance gains. Therefore, the non-binary SPC is proposed for LoRa to deal with noise-driven errors while maintaining low encoding complexity for the benefit of energy-efficient transmitters.

As presented in Figure 2, $PL+H$ bits are organized as M blocks with each block finally transmitted as $CR+4$ LoRa symbols. The SPC proposed uses one LoRa symbol from each of the M blocks to create a single-parity LoRa symbol. The resultant is $CR+4$ SPC parity symbols that constitute an additional block. The total number of blocks after SPC therefore becomes $M+1$ blocks.

For ease of notation, each LoRa symbol $s_k = k$ shall be referred to directly in terms of the index of the starting frequency offset k of the underlying basis function $\omega_k(nT)$. Accordingly, let $S = \{0,1,2,...,2^{SF}-1\}$ depict the set of possible LoRa symbols for a given spreading factor SF. Let us consider a message vector $P = [p_0, p_1, ..., p_{M-1}]$ comprised of M LoRa symbols where $p_m \in S$ depicts the LoRa symbol in the position $m = 0,1,...,M-1$ of the message P. Furthermore, let us encode the M symbols using a simple $M/M+1$ non-binary SPC code into a codeword $P' = [p_0, p_1, ..., p_{M-1}, p_M]$ such that the parity check symbol p_M is computed as

$$p_M = \left(\sum_{m=0}^{M-1} p_m\right) \mod 2^{SF}. \tag{11}$$

Let us now define $\mathcal{R} = [r_{k,m}]$, where $k = 0,1,...,2^{SF}-1$ and $m = 0,1,...,M$, as a two-dimensional matrix that signifies

[1]Figure 2: Influence of Coding Rate on Sensitivity in [14].

magnitudes of the 2^{SF} receiver correlator outputs corresponding to each of the $(M+1)$ constituent LoRa symbols in the encoded message P' assuming an AWGN channel. As presented by (5), the detected symbol in LoRa is selected as the index of the correlator output that exhibits the maximum correlation magnitude with the 2^{SF} possible LoRa basis functions. Let $D = [d_0, d_1, ..., d_M]$ depict the vector of detected LoRa symbols corresponding to the encoded message P' where $d_m \in S$ is evaluated as

$$d_m = \arg_k \max \left(r_{k,m}\right). \tag{12}$$

Error detection for the detected message D is conducted by the simple parity check using the addition of the detected message constituents as follows

$$h = \left(\sum_{m=0}^{M} d_m\right) \mod 2^{SF}, \tag{13}$$

where $h = 0$ presumes error-free communication, while $h \neq 0$ indicates an erroneous packet.

In order to pursue error correction whenever $h \neq 0$, it is necessary to evaluate the reliability of the detected message D. Such reliability could be assessed through the log-likelihood ratio (LLR) $L\left[D|\mathcal{R}\right]$ given as

$$L\left[D|\mathcal{R}\right] = \sum_{m=0}^{M} L\left[d_m|r_{d_m,m}\right], \tag{14}$$

where $0 < r_{d_m,m} < \infty$ and $r_{d_m,m}$ represents the correlator magnitude corresponding to detected symbol d_m at symbol position m in D. The LLRs $L[d_m|r_{d_m,m}]$ are given by

$$L\left[d_m|r_{d_m,m}\right] = \ln\left[\frac{\Pr\left[d_m = p_m|r_{d_m,m}\right]}{\Pr\left[d_m \neq p_m|r_{d_m,m}\right]}\right]. \tag{15}$$

By applying Bayes' rule and considering that an erroneous symbol corresponds to the selection of the correlator bin with the maximum complex Gaussian noise amplitude, $L[d_m|r_{d_m,m}]$ could be reformulated as

$$L\left[d_m|r_{d_m,m}\right] = \ln\left[\frac{f_\beta\left(r_{d_m,m}\right)}{\left(2^{SF}-1\right) \times f_{\hat{\rho}}\left(r_{d_m,m}\right)}\right], \tag{16}$$

where $f_\beta()$ corresponds to the probability density function of a Rician distribution with shape parameter $\kappa_\beta = E_S/N_0$ that governs the amplitude of a LoRa symbol transmitted with amplitude $\sqrt{E_S}$ over an AWGN channel, while $f_{\hat{\rho}}()$ is the density function for the distribution of the maximum of $2^{SF}-1$ identically Rayleigh distributed complex Gaussian noise amplitudes. Moreover, the multiplier of $2^{SF}-1$ in the denominator of (16) reflects the fact that each correlator output bin has an apriori probability of being a noise bin that is $2^{SF}-1$ folds more than of that being a LoRa symbol bin.

It has been shown in [15] that the Rician distribution with a shape parameter exceeding $10\,\mathrm{dB}$ may be approximated using a Gaussian distribution. Figure 1 in conjunction with (10) suggests that LoRa typically operates within the range of $E_S/N_0 > 15\,\mathrm{dB}$ to guarantee a BER performance that is better than 10^{-5}. Accordingly, $f_\beta(r_{d_m,m})$ in (16) may be approximated using a Gaussian distribution such that

$$f_\beta\left(r_{d_m,m}\right) = \frac{1}{\sqrt{2\pi\sigma^2}} \exp\left[-\frac{\left(r_{d_m,m} - \sqrt{E_S}\right)^2}{2\sigma^2}\right]. \tag{17}$$

Given $f_\beta(r_{d_m,m})$ from (17) and $f_{\hat{\rho}}(r_{d_m,m})$ derived from the differentiation of (8), $L[d_m|r_{d_m,m}]$ becomes expressed as

$$\begin{aligned} L\left[d_m|r_{d_m,m}\right] = A.\Big[&\tfrac{2r_{d_m,m}\sqrt{E_S}-E_S}{2\sigma^2} - \ln\left(r_{d_m,m}\right) - \\ &\left(2^{SF}-2\right).\ln\left(1-\exp\left[-\tfrac{r_{d_m,m}^2}{2\sigma^2}\right]\right)\Big], \end{aligned} \tag{18}$$

where $A = \left(2^{SF}-1\right)\sqrt{\frac{\sigma^2}{2\pi}}$. Substituting for (18) in (14), the composite reliability $L\left[D|\mathcal{R}\right]$ of the detected message before error correction could be evaluated.

For error correction, a list decoding approach is adopted that selects the most reliable corrected codeword assuming single erasure. Accordingly, let us define the set of valid codewords $\mathcal{V} = \{V^{(0)}, V^{(1)}, ..., V^{(M)}\}$ that includes $M+1$ candidate valid codewords. For each valid codeword $V^{(e)} \in \mathcal{V}$, $e = 0, 1, ..., M$, a single corrected symbol v_e replaces d_e assuming an erasure at position e in D such that

$$v_e = \sum_{m\,=\,0, m\,\neq\,e}^{M} d_m. \tag{19}$$

Therefore, for each valid codeword $V^{(e)} \in \mathcal{V}$, a new reliability measure $L[V^{(e)}|\mathcal{R}]$ is computed as

$$L\left[V^{(e)}|\mathcal{R}\right] = L\left[D|\mathcal{R}\right] - L\left[d_e|r_{d_e,e}\right] + L\left[v_e|r_{v_e,e}\right], \tag{20}$$

where $r_{v_e,e} < r_{d_e,e}$ signifies correlator output corresponding to the corrected LoRa symbol v_e and $L[v_e|r_{v_e,e}]$ is given as

$$L\left[v_e|r_{v_e,e}\right] = \ln\left[\frac{f_\beta\left(r_{v_e,e}\right)}{\left(2^{SF}-1\right) \times f_\rho\left(r_{v_e,e}\right)}\right], \tag{21}$$

where $f_\beta()$ remains to be approximated as a Gaussian distribution while $f_\rho()$ is the probability density function of the Rayleigh distribution of the magnitude of a single complex Gaussian noise amplitude. Therefore (21) is expressed as

$$L\left[v_e|r_{v_e,e}\right] = A.\left[\frac{2r_{v_e,e}\sqrt{E_S} - E_S}{2\sigma^2} - \ln\left(r_{v_e,e}\right)\right], \tag{22}$$

where A depicts the same constant as in (18).

The decoder would finally select the corrected codeword $C \in \mathcal{V}$ with the maximum reliability, i.e.,

$$C = V^{(c)} : c = \arg_e \max\left[L\left[V^{(e)}|\mathcal{R}\right]\right]. \tag{23}$$

B. SPC and LoRa Capacity

In LoRa, basis functions with different SF exhibit quasi-orthogonal characteristics [2]. Accordingly, LoRa supports coexistence of parallel logical networks corresponding to each available SF. In the following, each LoRa logical network shall be referred to as $SF^{(i)}$ network where $i \in \{7, 8, ..., 12\}$ is the network spreading factor. For any given $SF^{(i)}$ network, a simple ALOHA-based protocol is utilized for medium access over a set of available channels. End devices randomly select one of the available channels for each packet transmission. Accordingly, using the classical ALOHA formulas, the total successful LoRa throughput λ_S (packets/second) is given by

$$\lambda_S = \lambda.\sum_{i=7}^{12} \alpha^{(i)}.\exp\left[-\frac{\alpha^{(i)}\lambda T^{(i)}\left(M\right)}{N_C}\right], \tag{24}$$

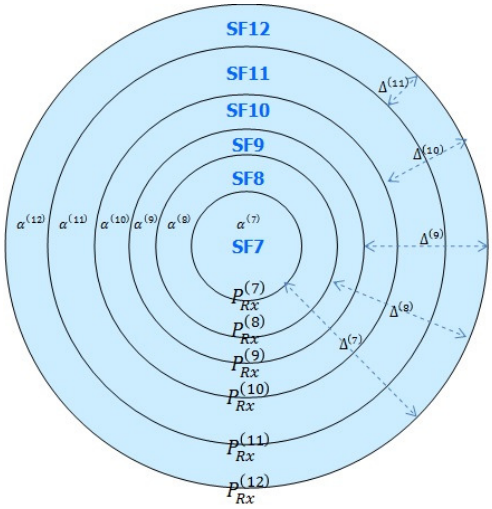

Fig. 3. LoRa SF Allocation Tiers based on Sensitivity.

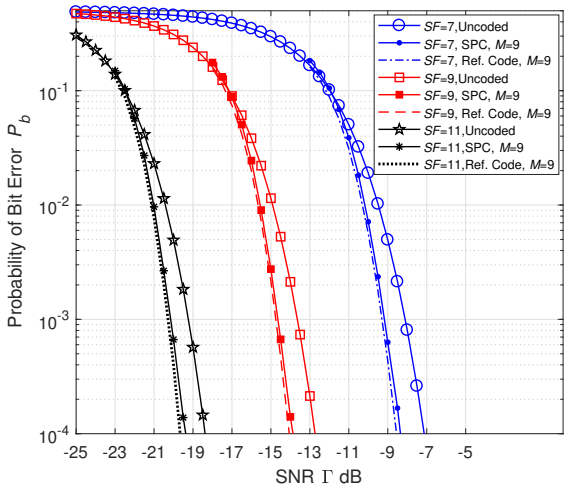

Fig. 4. LoRa BER Performance with SPC, $SF = 7, 9, 11$.

where λ is the total rate of packet arrivals to the LoRa network, $\alpha^{(i)}$ depicts the percentage of end devices within the $SF^{(i)}$ network (i.e., allocated with $SF = i$) and $T^{(i)}(M)$ is the transmission time (time-on-air) of the end devices' packets (constituted of M blocks) given $SF = i$ is used for communication. N_C depicts the number of channels available for communication where in LoRa the minimum number of mandatory channels is three.

A more relevant metric for applications supported by LoRa networks is the packet delivery ratio PDR [5]. The PDR is defined as the percentage of LoRa packets that are successfully received by the LoRa gateway and is given as

$$PDR = \sum_{i=7}^{12} \alpha^{(i)} . \exp\left[-\frac{\alpha^{(i)} \lambda T^{(i)}(M)}{N_C}\right]. \quad (25)$$

A typical approach for assigning end devices to an $SF^{(i)}$ network is based on sensitivity tiers as shown in Figure 3 [5], where each $SF^{(i)}$ network features a sensitivity $P_{Rx}^{(i)}$. SPC could potentially support an improved sensitivity of some given $SF^{(i)}$ network. The corresponding extension of the $SF^{(i)}$ network coverage radius leads to an increase in the allocation percentage $\alpha^{(i)}$ on the expense of that of the next tier $\alpha^{(i+1)}$. Moreover with the SPC coding rate of $M/M+1$, time-on-air for packet transmissions within $SF^{(i)}$ network increases to $T^{(i)}(M+1)$. The aggregate impact of the changes in $\alpha^{(i)}$, $T^{(i)}$ along with $\alpha^{(i+1)}$ on the PDR defined in (25) should determine whether or not SPC should be enabled within the $SF^{(i)}$ network. Let $X = [x^{(7)}, x^{(8)}, ..., x^{(12)}]$ depict a binary assignment vector to signify whether SPC is utilized in $SF^{(i)}$ network or not. In order to normalize the end devices' density, it shall be assumed that $x^{(12)} = 0$. Such normalization means that SPC is not utilized in the maximum tier network and the total LoRa network area remains constant. Let us now define $\Delta^{(i)}(M)$ as the sensitivity gap between $SF^{(i)}$ network and the maximum coverage $SF^{(12)}$ network expressed as

$$\Delta^{(i)}(M) = P_{Rx}^{(i)} - P_{Rx}^{(12)} - x^{(i)} \times CG^{(i)}(M), \quad (26)$$

where $P_{Rx}^{(i)}$ depicts the sensitivity of LoRa without SPC given $SF = i$ and $CG^{(i)}(M)$ is the coding gain for an SPC code with rate of $M/M+1$ with $SF = i$.

For an environment with uniformly distributed devices, the assignment percentage $\alpha^{(i)}$ could be derived from the ratio of the area of each tier relative to the area of the entire network environment. The total area of the network environment could be quantified in terms of the coverage radius of the minimum sensitivity $SF^{(12)}$ network. Given the sensitivity gap between the $SF^{(i)}$ network and the maximum coverage $SF^{(12)}$ network in (26), it is quite straightforward to show that $\alpha^{(i)}$ for the tier-assignment strategy in Figure 3 is given as

$$\alpha^{(i)} = \begin{cases} 10^{-\frac{2\Delta^{(i)}(M)}{10\varepsilon}} & i = 7 \\ 10^{-\frac{2\Delta^{(i)}(M)}{10\varepsilon}} - 10^{-\frac{2\Delta^{(i-1)}(M)}{10\varepsilon}} & 7 < i \leq 12 \end{cases}, \quad (27)$$

where in (27), $\Delta^{(12)} = 0$ and ε is the pathloss exponent.

The problem formulation for SPC optimization reverts to the vector $X = [x^{(7)}, x^{(8)}, ..., x^{(11)}, 0]$ that maximizes

$$PDR = \sum_{i=7}^{12} \left(1 - x^{(i)}\right) \times \alpha^{(i)} . \exp\left[-\frac{\left(1 - x^{(i)}\right) \lambda T^{(i)}(M)}{N_C}\right] + \sum_{i=7}^{12} x^{(i)} \times \alpha^{(i)} . \exp\left[-\frac{x^{(i)} \lambda T^{(i)}(M+1)}{N_C}\right]. \quad (28)$$

IV. Simulation Results

A. Coding Gain of SPC in LoRa

In order to evaluate the ability of SPC to deal with noise-driven errors in LoRa modulation, Figure 4 presents the simulated BER performance of LoRa using SPC assuming a coding rate of $M/M+1 = 0.9$. The SPC BER curves are compared against the uncoded BER performance from Figure 1. It is evident that SPC renders measurable coding gains across the range of LoRa spreading factors. In order to further assess the SPC error correction capabilities, the BER is also referenced against a theoretical FEC code with single symbol error correction capability. It is evident from Figure 4 that the devised SPC is virtually correcting all single symbol errors. Figure 5 presents the attained coding gains of SPC as a function of the coding rate. The simulated ranges for $M = 4$ to

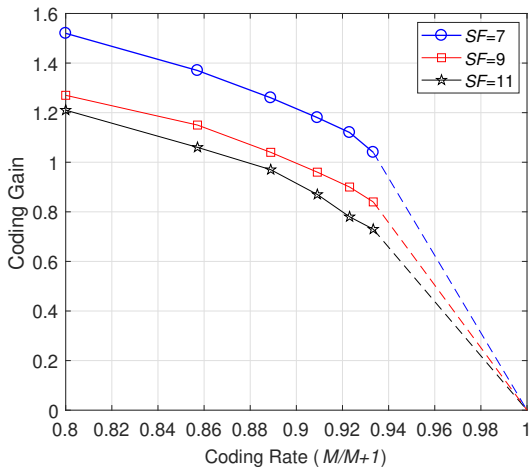

Fig. 5. Coding gain of SPC versus coding rate at $SF = 7, 9, 11$.

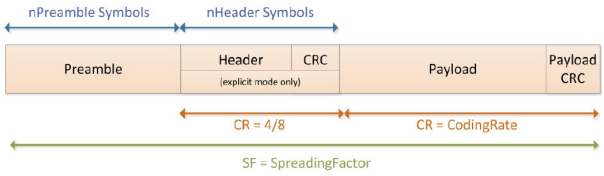

Fig. 6. LoRa Packet Format [14].

$M = 14$ correspond to coding rates between 0.8 to 0.933. For simulation time restrictions at larger values of M, the dashed lines in Figure 4 exhibit a linear extrapolation for the decay of the coding gain until it reaches 0 as $M \to \infty$. The decrease in coding gain is due to the decreased probability of single symbol error (SPC correction capability) with increasing M.

B. LoRa Capacity with SPC Optimization

In the following, we shall evaluate LoRa capacity under SPC for a home security application as an illustrative example of one of the typical candidate applications within LP-WAN. For the home security application under study, the application payload is assumed to be 20 bytes with one packet generated every 10 minutes [16]. Furthermore, an urban environment is assumed with a pathloss exponent given as $\varepsilon = 2.65$ as estimated in [17]. As per (28), the packet delivery ratio PDR is dependent on the assignment percentage $\alpha^{(i)}$ and transmission times $T^{(i)}(M)$, $T^{(i)}(M+1)$ (without, with SPC respectively) in conjunction with the SPC assignment vector X. As indicted by (26), (27), the assignment percentage $\alpha^{(i)}$ could be derived from the coding gain curves in Figure 5. The transmission times $T^{(i)}(M)$, $T^{(i)}(M+1)$ on the other hand are dependent on the number of LoRa symbols required to transmit the LoRa packet that is used to carry the application data payload. The nominal LoRa packet format is shown Figure 6. The packet is comprised of a preamble for synchronization followed by the physical layer header, payload along with an optional CRC [14]. While the number of preamble symbols could be programmable, the number of LoRa symbols to represent the remaining physical layer packet depends on the coding rate and spreading factor used among other parameters. In [14], the number of preamble symbols are set as $L_{Preamble} = 4.25 + L_{Prog}$ where L_{Prog} is the number of programmable symbols. The number of

TABLE II
LoRa Parameters for Reference Scenario.

B (kHz)	N_C	$L_{preamble}$	CR	CRC	IH	DE	PL
125	3	12.25	1	1	0	0	33

TABLE III
SPC Parameters for Reference Scenario.

SF	M	SPC Code Rate	Total Code Rate	Coding Gain (dB)
7	10	0.909	0.727	1.18
8	9	0.9	0.72	1.18
9	8	0.899	0.711	1.04
10	7	0.875	0.7	1.025
11	6	0.857	0.686	1.03
12	6	1	0.8	0

LoRa symbols corresponding to the physical layer packet is governed by $L_{phy-payload}[M] = 8 + M \times (CR + 4)$ where the number of blocks M is calculated in [14] as

$$M = \max\left(\left\lceil \frac{8PL - 4SF + 28 + 16CRC - 20IH}{4(SF - 2DE)} \right\rceil, 0\right). \quad (29)$$

where $\lceil\rceil$is the ceiling function, PL is the MAC layer payload (in bytes) that includes the MAC header and the application data, SF is the spreading factor, $CRC = 1$ if the optional CRC is enabled, $IH = 1$ means implicit header (i.e. physical layer header not transmitted) is enabled and $DE = 1$ indicates that a data optimization feature is activated. Accordingly, the transmission time assuming no SPC is used is given by

$$T^{(i)}(M) = \frac{B}{2^{SF}} \times \left[L_{Preamble} + L_{phy-payload}[M]\right]. \quad (30)$$

When SPC is activated the physical layer payload is slightly extended such that $L_{phy-payload}[M+1] = 8 + (M+1) \times (CR+4)$.

The LoRa parameters used for the reference scenario are shown in Table II. It is to be noted that for the home security application under study with 20 bytes of application data, $PL = 33$ bytes since the MAC header in LoRa is typically 13 bytes. Table III lists the number of blocks M within each LoRa packet in absence of SPC as per (29) for all values of SF. The table also displays the coding rates, gains that are associated with each spreading factor if SPC is enabled.

Figure 7 shows the PDR with increasing number of end devices for the nominal LoRa case compared against the PDR with SPC optimization assuming $CR = 1$. The optimal configuration in Figure 7 is achieved with the help of a full search of all 2^5 possible configurations of the SPC assignment vector X. When inspecting the optimal configurations of X, it has been apparent that for different spreading factors the SPC is enabled at low loads and tend to be disabled with increasing loads. This is shown in Figure 7 by the vertical lines that indicate the number of end devices after which SPC is disabled for a given SF. It is evident that at low loads SPC activation is beneficial. With increasing load SPC is disabled starting within the $SF^{(11)}$ network until SPC in both $SF^{(7)}$ $SF^{(8)}$ networks are disabled simultaneously for the listed example.

In order to evaluate the LoRa capacity, let us set a target PDR of 90% [4]. Figure 8 compares the capacity of the nominal LoRa against the capacity of LoRa with SPC optimization assuming $CR = 1$ (i.e., Hamming code rate

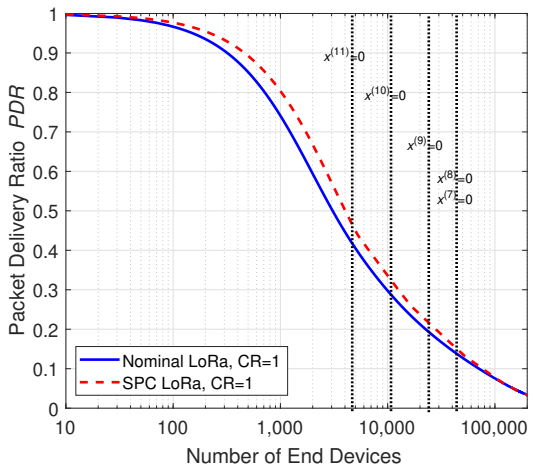

Fig. 7. PDR versus number of end devices with/without SPC Optimization.

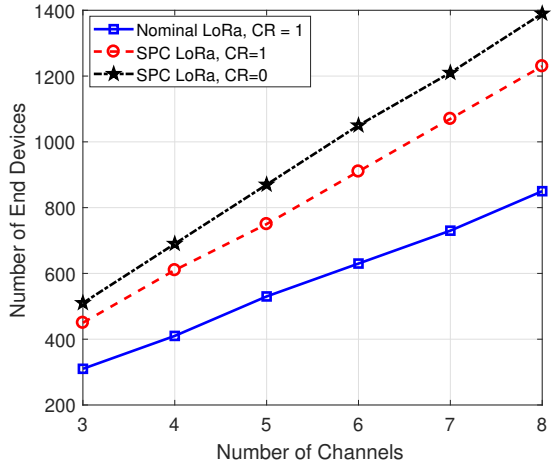

Fig. 8. Capacity Gain of LoRa with SPC Optimization.

of $4/5$ to handle synchronization errors). It is evident that SPC can offer capacity improvements at the scale of roughly 50% across all ranges of number of LoRa channels presented. Figure 8 also includes a more aggressive scenario with the setting of $CR = 0$. In this case, it is presumed that SPC will be called upon to address both synchronization errors and noise-driven errors. The results presented in Figure 8 indicate that additional capacity gains are achievable such that overall gain becomes at the scale of 65%.

V. Conclusions

This paper has proposed SPC as a tool for enhancing LoRa capacity. By enabling and disabling SPC, it is possible to tradeoff system loads against time-on-air across the logical spreading factor networks of LoRa. It is shown that in fact SPC optimization has the potential of enhancing the LoRa capacity by up to 65% for one typical LP-WAN application such as home security. In future work, iterative decoding techniques could be deployed between non-binary SPC and binary LoRa Hamming codes to further enhance coding gains. Moreover, an optimization algorithm could be devised to combine SPC optimization with SF-allocation where assignment distances do not necessarily coincide with sensitivity distances.

Acknowledgment

This work has been supported by the Alexander von Humboldt Foundation in Germany.

References

[1] M. Centenaro, L. Vangelista, A. Zanella, and M. Zorzi, "Long-range communications in unlicensed bands: The rising stars in the IoT and smart city scenarios," *IEEE Wireless Communications*, vol. 23, no. 5, pp. 60–67, 2016.

[2] D. Croce, M. Gucciardo, S. Mangione, G. Santaromita, and I. Tinnirello, "Impact of lora imperfect orthogonality: Analysis of link-level performance," *IEEE Communications Letters*, vol. 22, no. 4, pp. 796–799, April 2018.

[3] O. Georgiou and U. Raza, "Low power wide area network analysis: Can lora scale?" *IEEE Wireless Communications Letters*, vol. 6, no. 2, pp. 162–165, April 2017.

[4] M. C. Bor, U. Roedig, T. Voigt, and J. M. Alonso, "Do lora low-power wide-area networks scale?" in *Proceedings of the 19th ACM International Conference on Modeling, Analysis and Simulation of Wireless and Mobile Systems*, ser. MSWiM '16. New York, NY, USA: ACM, 2016, pp. 59–67. [Online]. Available: http://doi.acm.org/10.1145/2988287.2989163

[5] F. V. den Abeele, J. Haxhibeqiri, I. Moerman, and J. Hoebeke, "Scalability analysis of large-scale lorawan networks in ns-3," *IEEE Internet of Things Journal*, vol. 4, no. 6, pp. 2186–2198, Dec 2017.

[6] A. Augustin, J. Yi, T. Clausen, and W. M. Townsley, "A study of lora: Long range and low power networks for the internet of things," *Sensors*, vol. 16, no. 9, 2016. [Online]. Available: http://www.mdpi.com/1424-8220/16/9/1466

[7] F. Cuomo, M. Campo, A. Caponi, G. Bianchi, G. Rossini, and P. Pisani, "Explora: Extending the performance of lora by suitable spreading factor allocations," in *2017 IEEE 13th International Conference on Wireless and Mobile Computing, Networking and Communications (WiMob)*, Oct 2017, pp. 1–8.

[8] J. T. Lim and Y. Han, "Spreading factor allocation for massive connectivity in lora systems," *IEEE Communications Letters*, vol. 22, no. 4, pp. 800–803, April 2018.

[9] P. J. Marcelis, V. Rao, and R. V. Prasad, "Dare: Data recovery through application layer coding for lorawan," in *Proceedings of the Second International Conference on Internet-of-Things Design and Implementation*, ser. IoTDI '17. New York, NY, USA: ACM, 2017, pp. 97–108. [Online]. Available: http://doi.acm.org/10.1145/3054977.3054978

[10] L. Vangelista, "Frequency shift chirp modulation: The LoRa modulation," *IEEE Signal Processing Letters*, vol. 24, no. 12, pp. 1818–1821, 2017.

[11] O. Bernard, A. Seller, and N. Sornin, "Low power long range transmitter," Semtech Corporation, Camarillo, CA 93012, 2015. Application Number 13154071.8/EP20130154071, Publication Number EP2763321 A1.

[12] M. Knight and B. Seeber, "Decoding lora: Realizing a modern lpwan with sdr," *Proceedings of the GNU Radio Conference*, vol. 1, no. 1, 2016. [Online]. Available: https://pubs.gnuradio.org/index.php/grcon/article/view/8

[13] Semtech application note an1200.22, "lora modulation basics," revision 2, semtech corporation, may 2015. [Online]. Available: https://www.semtech.com/uploads/documents/an1200.22.pdf

[14] Semtech application note an1200.13, "sx1272/3/6/7/8 lora modem designer's guide," revision 1, semtech corporation, july 2013. [Online]. Available: http://www.semtech.com/images/datasheet/LoraDesignGuide_STD.pdf

[15] R. D. Nowak, "Wavelet-based Rician noise removal for magnetic resonance imaging," *IEEE Transactions on Image Processing*, vol. 8, no. 10, pp. 1408–1419, 1999.

[16] K. Mikhaylov, . J. Petaejaejaervi, and T. Haenninen, "Analysis of capacity and scalability of the lora low power wide area network technology," in *European Wireless 2016; 22th European Wireless Conference*, May 2016, pp. 1–6.

[17] P. Jorke, S. Bocker, F. Liedmann, and C. Wietfeld, "Urban channel models for smart city iot-networks based on empirical measurements of lora-links at 433 and 868 mhz," in *2017 IEEE 28th Annual International Symposium on Personal, Indoor, and Mobile Radio Communications (PIMRC)*, Oct 2017, pp. 1–6.